Biogeosciences, 12, 6515–6528, 2015
www.biogeosciences.net/12/6515/2015/
doi:10.5194/bg-12-6515-2015

Biogeosciences Open Access EGU

Production regime and associated N cycling in the vicinity of Kerguelen Island, Southern Ocean

A. J. Cavagna[1], F. Fripiat[1], M. Elskens[1], P. Mangion[2], L. Chirurgien[3], I. Closset[4], M. Lasbleiz[3], L. Florez-Leiva[5,6], D. Cardinal[4], K. Leblanc[3], C. Fernandez[7,8], D. Lefèvre[3], L. Oriol[8], S. Blain[8], B. Quéguiner[3], and F. Dehairs[1]

[1]Analytical, Environmental and Geo-Chemistry dept. (AMGC), Earth System Sciences Research Group, Vrije Universiteit Brussel, Brussels, Belgium
[2]Centre for Coastal Biogeochemistry Research, Southern Cross University, Lismore, Australia
[3]Aix-Marseille Université, Université de Toulon, CNRS/INSU, IRD, MIO, UM110, 13288, Marseille, CEDEX 09, France
[4]Sorbonne Universités, UPMC, LOCEAN Laboratory, 4 place Jussieu, 75005 Paris, France
[5]Program of Oceanography, University of Antioquia, Medellin, Colombia
[6]Program of Biology, University of Magdalena, Santa Marta, Colombia
[7]Department of Oceanography, COPAS SurAustral program and Interdisciplinary Center for Aquaculture Research (INCAR), University of Concepción, Chile
[8]Sorbonne Universités, UPMC, UMR7621, Laboratoire d'Océanographie Microbienne, Observatoire Océanologique, 66650 Banyuls/mer, France

Correspondence to: A. J. Cavagna (acavagna@vub.ac.be)

Received: 22 November 2014 – Published in Biogeosciences Discuss.: 19 December 2014
Accepted: 13 October 2015 – Published: 13 November 2015

Abstract. Although the Southern Ocean is considered a high-nutrient, low-chlorophyll (HNLC) area, massive and recurrent blooms are observed over and downstream of the Kerguelen Plateau. This mosaic of blooms is triggered by a higher iron supply resulting from the interaction between the Antarctic Circumpolar Current and the local bathymetry. Net primary production, N uptake (NO_3^- and NH_4^+), and nitrification rates were measured at eight stations in austral spring 2011 (October–November) during the KEOPS 2 cruise in the Kerguelen Plateau area. Natural iron fertilization stimulated primary production, with mixed layer integrated net primary production and growth rates much higher in the fertilized areas (up to 315 mmol C m^{-2} d^{-1} and up to 0.31 d^{-1} respectively) compared to the HNLC reference site (12 mmol C m^{-2} d^{-1} and 0.06 d^{-1} respectively). Primary production was mainly sustained by nitrate uptake, with f ratios (corresponding to NO_3^--uptake / (NO_3^--uptake + NH_4^+-uptake)) lying at the upper end of the observations for the Southern Ocean (up to 0.9). We report high rates of nitrification (up to ~ 3 µmol N L^{-1} d^{-1}, with ~ 90 % of them < 1 µmol N L^{-1} d^{-1}) typically occurring below the euphotic zone, as classically observed in the global ocean. The specificity of the studied area is that at most of the stations, the euphotic layer was shallower than the mixed layer, implying that nitrifiers can efficiently compete with phytoplankton for the ammonium produced by remineralization at low-light intensities. Nitrate produced by nitrification in the mixed layer below the euphotic zone is easily supplied to the euphotic zone waters above, and nitrification sustained 70 ± 30 % of the nitrate uptake in the productive area above the Kerguelen Plateau. This complicates estimations of new production as potentially exportable production. We conclude that high productivity in deep mixing system stimulates the N cycle by increasing both assimilation and regeneration.

1 Introduction

The Southern Ocean is considered a high-nutrient, low-chlorophyll (HNLC) system due to a combination of several factors, which include upwelling of nutrient-rich waters south of the Antarctic polar front and a combined iron and light co-limitation of phytoplankton growth (Martin, 1990; Falkowski et al., 1998; Sarmiento et al., 2004). The South-

ern Ocean is also recognized as a major hotspot for gas exchanges and accounts for up to 20 % of the global ocean CO_2 uptake (Takahashi et al., 2009). Concerns regarding ongoing climate change have triggered great interest in this part of the global ocean (Le Quéré et al., 2007).

Since the "iron hypothesis" formulated in the early nineties by Martin (1990) the last 2 decades have witnessed an exponential increase in interest of the scientific community in iron availability and associated biological processes. The aim was to explore the role of iron in enhancing the biological pump and the subsequent increase in the drawdown of atmospheric CO_2. Numerous artificial iron-enrichment experiments (see Boyd et al., 2007) were conducted in situ to explore the fertilization effect of iron (de Baar et al., 2005, 2008; Boyd et al., 2007; Smetacek et al., 2012; Quéguiner, 2013). In parallel, several naturally iron-enriched sites were studied (e.g. Boyd et al., 2007) to understand the mechanisms driving such iron fertilization and their impacts on biogeochemical systems without external forcing (Blain et al., 2007, 2008; Pollard et al., 2007, 2009; Bowie et al., 2011). The KEOPS project, carried out in the Kerguelen area, is dedicated to the understanding of naturally iron-fertilized systems functioning over a large spatial and seasonal scale. For that purpose a first cruise was completed during austral summer 2005 (KEOPS1, February–March; Blain et al., 2007) and a second cruise was completed during austral spring 2011 (KEOPS2, October–November 2011).

Through its crustal interface the Kerguelen area (composed of Kerguelen Island, the Kerguelen Plateau, and Heard Island in the south-east) enriches the surrounding waters with macronutrients and trace elements. It also strongly impacts the local oceanic physical dynamics due to its island mass effect (Doty and Oguri, 1956). The interactions between geostrophic water flow disturbances due to the presence of the island, the tidal activity over the plateau, and the strong winds characterizing the area generate internal waves, eddies, jets, Ekman pumping, and a complex hydrodynamical environment (Heywood et al., 1990; Park et al., 2008; Gille et al., 2014). These characteristics are key factors inducing the fertilization and the associated higher productivities around the Kerguelen Island area as compared to the HNLC surrounding waters (Blain et al., 2001, 2007; Fig. 1). Moreover, a third condition impacting productivity is the proximity of the polar front, the trajectory of which is steered by the bottom topography (Park et al., 2014). Such a frontal system by itself offers peculiar conditions inducing significant biological activity (de Baar et al., 1995).

Here we report net primary production together with N uptake (NO_3^- and NH_4^+) and nitrification rates over the Kerguelen Plateau and the downstream area visited during KEOPS-2. Studies conducted during KEOPS1 showed a decoupling of the seasonal use of nitrate and silicic acid stocks over the Kerguelen Plateau (Mosseri et al., 2008), although $Si : NO_3$ assimilation ratios were close to 1, in accordance with what is expected for non-limiting iron conditions (Takeda, 1998; Hutchins and Bruland, 1998). Mosseri et al. (2008) attributed this peculiar decoupling to the capacity of diatoms to grow on ammonium that could result from high heterotrophic activity at the end of the productive season. These observations highlight the potential importance of nitrogen recycling in the surface layer. In this context, the objectives of the studies undertaken during KEOPS2 were

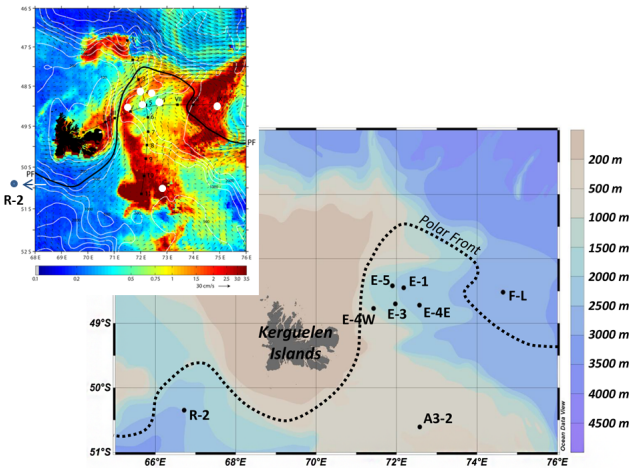

Figure 1. Map of the KEOPS 2 cruise area (Indian sector of the Southern Ocean) showing the location of stations discussed in the study, courtesy of Ivia Closset. Dotted line represents the position of the polar front from Park et al. (2014). The inset picture gives indication about surface chl *a* (colour scale), surface velocity fields (arrows), and the polar front (PF, black line). Black dots in the inset picture represent KEOPS 2 transect stations which were not considered in this study; stations for which we performed incubations are represented by the white circles: the bloom stations over the Kerguelen Plateau (E4-W and A3-2) and north of the polar front (F-L) and the meander stations (E stations). The reference HNLC station (R-2) lies outside the area covered by the map (66.69° E, 50.39° S). This satellite picture corresponds to the last week of the KEOPS2 cruise. Courtesy of Y. Park and colleagues.

1. to evaluate and compare the C- and N-assimilation rates during austral spring over the Kerguelen Plateau, in the wake of Kerguelen Island, and at a reference HNLC site;

2. to assess the importance of recycling processes for the supply of nitrogen sources for phytoplankton in the surface layer;

3. to test the intensity of nitrification and its role in the recycling of nitrogen.

2 Materials and methods

The KEOPS 2 expedition took place in the Indian sector of the Southern Ocean during early spring 2011 (September to November) on board the R/V *Marion Dufresne*. Process studies were conducted at eight sites (Fig. 1), including

a reference station (R-2) in a HNLC off-plateau region located south-west of the Kerguelen Islands, one station (A3-2) above the Plateau, one station (E4-W) on the Plateau margin, one station (F-L) north of the polar front to the east of Kerguelen, and four further stations (E-1, E-3, E4-E, E-5) in a complex recirculation system of a stationary meander confined by the polar front.

At these eight sites we performed isotope tracer experiments to assess the following rates:

- C-fixation rates (hereafter defined as net primary production) by spiking with ^{13}C-DIC and subsequent measurement of the ^{13}C incorporation into biomass;
- ammonium and nitrate uptake rates by spiking either with $^{15}N–NH_4^+$ or $^{15}N–NO_3^-$ and subsequent measurement of the ^{15}N incorporation into biomass;
- nitrification rates by spiking with $^{15}N–NO_3^-$ and measuring the ^{14}N isotopic dilution of ^{15}N-nitrate resulting from the oxidation of both ammonium and nitrite by the nitrifiers. This allows us to assess the second step in the nitrification process (i.e. nitrate production).

Surface waters were sampled at seven to eight depths corresponding to 75, 45, 25, 16, 4, 1, 0.3, 0.01 % of the surface photosynthetically active radiation (PAR), using Niskin bottles mounted on a rosette fitted with a PAR sensor. For each light level, two acid-cleaned 1L polycarbonate incubation bottles were filled with seawater. The two bottles were spiked with 200 µmol L^{-1} of $^{13}C–HCO_3^-$ (99 atom ^{13}C %), corresponding to a tracer addition equivalent of ≈ 10 % of the surface seawater DIC concentration (≈ 2 mM) and providing a duplicate of net primary production. One of the bottles was spiked with $^{15}N–NO_3^-$ and the other with $^{15}N–NH_4^+$ (98 atom ^{15}N %). The amount of spike added was calculated taking into account the original nitrate and ammonium concentrations in order to achieve concentration increments < 10 %. This required nutrient concentration level to be available, as obtained from the analysis of preceding CTD casts. Nitrate was measured by continuous flow analysis (Aminot and Kérouel, 2007) and ammonium via fluorometric method (Holmes et al., 1999). The continuous flow approach accuracy was assessed using reference material (Certipur, Merck). The precisions were in the range of 1–4 % and the limit of detection was 0.02 µM for NO_3^- and NO_2^- (see also Blain et al., 2015).

Incubation bottles were then transferred into on-deck incubators, cooled with circulating surface seawater, and wrapped in neutral density screens simulating the photometric depths. Incubation experiments were stopped after 24 h. This relatively long incubation time implies that we probably underestimated uptake rates in case of (1) release of ^{15}N and ^{13}C to the dissolved organic pool during the course of the experiment (Bronk et al., 1994; Laws et al., 2002) and (2) ammonification, which would result in diluting the ^{15}N-spiked ammonium pool with ^{14}N. By applying a steady-state model (Glibert et al., 1982) assuming that uptake and regeneration rates are equal for each nitrogen pool, which should be the case here given the low and relatively constant concentration of ammonium, the factor by which ammonium uptake rates are underestimated is 1.17 ± 0.23 (1 SD; minimum = 1.00; maximum = 2.36). This is in the range of factors (1.5 to 2.0) suggested by Rees et al. (1995), Elskens et al. (1997), and Slawyk et al. (1997). Also, there is no significant effect on the estimation of the f ratio (i.e. NO_3^- uptake / (NO_3^- uptake + NH_4^+ uptake; Dugdale and Goering, 1967), as the relationship between the uncorrected and corrected f ratio is close to 1 (0.96 ± 0.01; $R^2 = 0.99$, p value < 0.001). Given the low underestimation, uncorrected ammonium uptake rates will be presented and discussed. Moreover, we opted for long incubation times in order to enhance sensitivity for detection of nitrification and to enable the comparison with Si uptake and dissolution experiments carried out over similar 24 h periods (Closset et al., 2014).

Both at the initial and final incubation times (initial time meaning just after spiking), subsamples for nitrate (10 mL) and ammonium concentrations (2 × 20 mL) were directly measured. A further additional 10 mL were sampled from the $^{15}N–NO_3^-$ incubation bottle at initial and final time for assessment of initial and final ^{15}N-nitrate conditions. These subsamples were filtered using 0.2 µm Acrodisc filters (Sartorius) and stored at −20 °C for later analysis of nitrate isotopic composition. The remaining seawater was filtered on pre-combusted (450 °C) glass fiber filters (Sartorius, MGF, nominal porosity 0.7 µm, 25 mm diameter). Filters were placed in pre-combusted scintillation vials, dried at 50 °C, and stored in the dark at room temperature until further analysis at the home-based laboratory.

Particulate organic nitrogen (PON) and particulate organic carbon (POC) concentrations along with their ^{15}N and ^{13}C abundances (atom ^{13}C and ^{15}N %) were analysed via an elemental analyser-isotope ratio mass spectrometer (EA-IRMS) using the method described in Savoye et al. (2004).

Atom ^{15}N % for nitrate at initial and final time was measured using the denitrifier method (Sigman et al., 2001). Briefly, 20–30 nmol of nitrate was quantitatively converted to N_2O gas by denitrifying bacteria (*Pseudomonas aureofaciens*) that lack an active N_2O reductase. The ^{15}N abundance of the N_2O was measured by gas chromatography/isotope ratio mass spectrometry (GC/IRMS) with online cryotrapping.

C-assimilation and ammonium uptake rates (ρNH_4^+) were calculated from the equations of Dugdale and Goering (1967) where atom % ^{13}DIC t_i and atom %$^{15}NH_4^+$ t_i were calculated and the other parameters were measured. For C-fixation this equation is

$$V = \frac{(\text{atom\%}^{13}\text{C}_{\text{POC tf}})}{\text{time} \cdot (\text{atom\%}^{13}\text{C}_{\text{DIC t}_i})}, \quad (1)$$

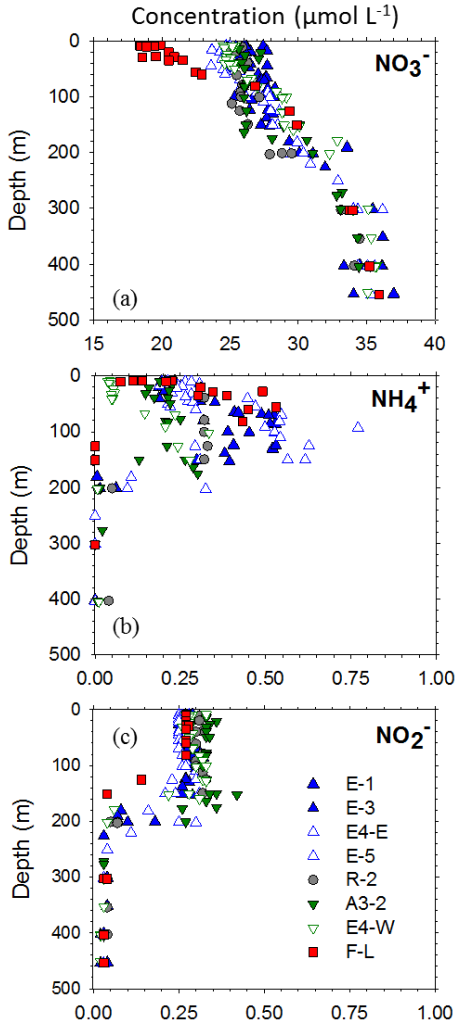

Figure 2. Nitrate **(a)**, ammonium **(b)**, and nitrite **(c)** concentration ($\mu mol\,L^{-1}$) vs. depth (m). See Supplement for detailed $[NH_4^+]$ vertical profiles and associated MLD per station.

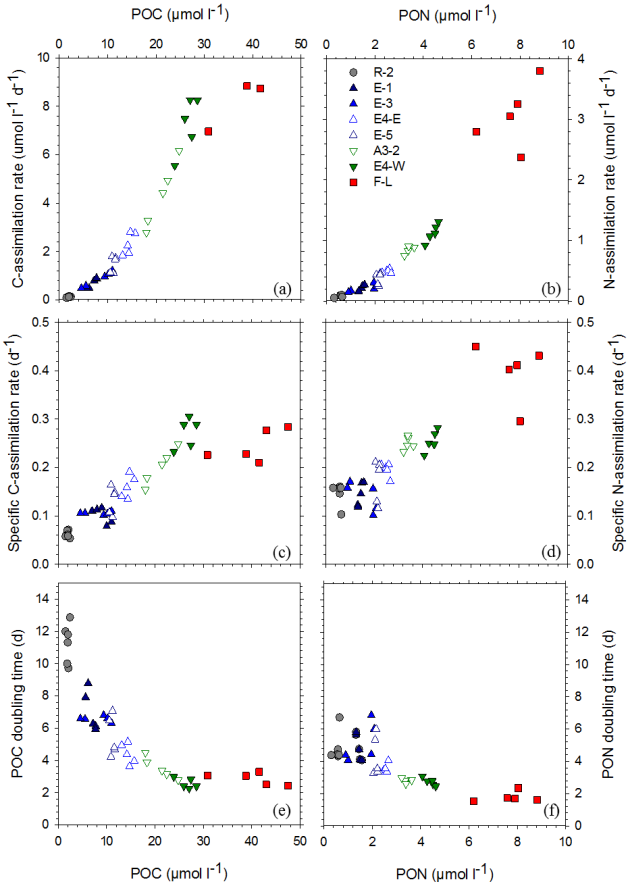

Figure 3. Euphotic layer (100 to 1 % PAR) relationship between **(a)** POC and NPP, also called the C-assimilation rate ($\mu mol\,C\,m^{-2}\,d^{-1}$); **(b)** PON ($\mu mol\,L^{-1}$) and N-assimilation rates ($\mu mol\,N\,m^{-2}\,d^{-1}$); **(c)** POC and specific C-assimilation rate (growth rate; d^{-1}); **(d)** PON and specific N-assimilation rate (growth rate; d^{-1}); **(e)** POC and POC doubling time; **(f)** PON and PON doubling time.

$$NPP = [POC_{tf}] \cdot V, \quad (2)$$

where V is the specific C-assimilation rate (in d^{-1}), NPP is net primary production (in $\mu mol\,C\,L^{-1}\,d^{-1}$), atom $\%^{13}C$ is the measured abundances minus the natural abundances, and t_f and t_i refer to the final and initial time of incubation respectively. Except for nitrate for which initial abundances were measured, the initial abundances for both DIC and NH_4^+ were calculated by taking into account the spike addition and isotopic abundance.

The nitrate uptake rate (ρNO_3^-) was first corrected for the isotope dilution effect during incubation and then assessed with the following equations (Nelson and Goering, 1977a, b):

$$VNO_3^- = \frac{\text{atom}\%^{15}N_{PONt_f}}{\text{time} \cdot \sqrt{\text{atom}\%^{15}NO_{3t_i}^- \cdot \text{atom}\%^{15}NO_{3tf}^-}}, \quad (3)$$

$$\rho NO_3^- = [PON_{tf}] \cdot VNO_3^-. \quad (4)$$

The nitrification (RNO_3^-) rate was assessed using the integrated rate equation of the Blackburn model (Blackburn, 1979; Elskens et al., 2005):

$$RNO_3^- = \frac{\ln\left(\text{atom}\%^{15}NO_{3t_i}^- / \text{atom}\%^{15}NO_{3tf}^-\right) \cdot \left[NO_{3tf}^- - NO_{3t_i}^-\right]}{\text{time} \cdot \left(\left[NO_{3tf}^-\right] / \left[NO_{3t_i}^-\right]\right)}. \quad (5)$$

The uncertainties on uptake (NPP, ρNH_4, and ρNO_3) and nitrification (RNO_3) rates were assessed using Monte-Carlo simulations assuming normal distributions for all variables.

The modelled nitrification rates were screened for consistency between observed evolutions of nitrate concentrations over the duration of the incubation experiment and measured nitrate uptake rates. The difference between nitrate uptake and nitrification should be compatible with the change in nitrate concentration over the duration of the incubation experiment, taking into account a 10 % precision (relative standard deviation, SD) on rates and concentrations measurements. When the rates given by the model were incompatible with temporal evolution of nitrate concentration, nitrification experiments were considered to be flawed and were left out of the data set. We point out that measuring nitrification rates under conditions of high ambient nitrate is methodologically challenging. Indeed, because ambient nitrate is high, sensitivity is poor. The latter is estimated at 0.26 µmol L^{-1} d^{-1} considering how much nitrification is needed to change the isotopic composition of the nitrate pool by 2 SD. Furthermore, the measurement precision ($\pm$0.26 µmol L^{-1} d^{-1}; estimated by taking into account the precision on the isotopic measurement; 2 SD) is poor. We note that such values for sensitivity and precision of nitrification rates analysis exceed most of the nitrification rates reported to date for the open ocean (Ward, 2008).

3 Results

Except for station (F-L) north of the polar front, the different water masses and associated biogeochemical properties were characteristic of the Antarctic Zone: relatively warmer waters in the upper mixed layer (defined following the density criterion of 0.02 kg m^{-3}; de Boyer Montégut et al., 2004) and the remnants of winter water in the lower part of the mixed layer (temperature minimum layer; Park et al., 2008). South of the polar front, mixed layer macronutrient levels were high and their distributions were relatively uniform between stations (Blain et al., 2015; Closset et al., 2014), with an average nitrate concentration of $\sim$ 25 µmol L^{-1} (Fig. 2a). In agreement with a scenario of progressive nutrient consumption during meridional water transfer northward across the Antarctic Circumpolar Current (Sigman et al., 1999; Sarmiento et al., 2004), the station north of the polar front (F-L) had higher surface temperatures (1 to 2 °C; data not shown) and lower nitrate concentrations (Fig. 2a). Both ammonium and nitrite concentrations in the mixed layer were low and remained relatively constant over time ($\sim$ 0.25 µmol L^{-1}), indicating a tight balance between production and consumption processes (Fig. 2b, c, and Supplement). There is, however, an exception for station F-L north of the polar front where a gradient in ammonium concentration was observed within the mixed layer. This contrasts most stations where an ammonium accumulation (up to 0.5 µmol L^{-1}) was observed below the mixed layer (Fig. 2b). An ammonium accumulation probably results from an imbalance between ammonium production (remineralization) and consumption processes (assimilation + nitrification) (Blain et al., 2015).

Both POC and PON concentrations increased from the HNLC reference station (R-2) to the meander stations (E stations) and then to the high productive sites, over the southeastern Kerguelen Plateau (A3-2) and at the margin (E4-W) as well as further north of the polar front (F-L) (Fig. 3). Overall, this spatial distribution of phytoplankton biomass is in agreement with satellite chlorophyll-a (Chl-a) observations (Fig. 1). A positive relationship is apparent between biomass (µmol L^{-1}) and assimilation rates (µmol L^{-1} d^{-1}), as well as specific uptake rate (V; d^{-1}; growth rate) both for carbon and nitrogen (Fig. 3a, b, c, d). Therefore a negative relationship holds between biomass and doubling time ($T_d = \ln(2)/V$; in days) (Fig. 3e, f). The bloom over the Kerguelen Plateau (A3-2 and E4-W) and north of the polar front (F-L) presented higher assimilation rates per unit of C and N biomass than the stations in the HNLC area (R-2) and the meander (E stations).

In general, vertical profiles of net primary production followed light availability in the mixed layer, with a sharp decrease below the euphotic layer depth (Zeu; 1 % surface PAR depth) (Fig. 4). Primary production extended well below Zeu, although at much lower rates than at shallower depths. This was particularly obvious for the most productive stations; primary production rates were still 0.36, 0.37, and 0.12 µmol C L^{-1} d^{-1} at the 0.3 % PAR level, as compared to rates of 11.9, 8.3, and 6.2 µmol C L^{-1} d^{-1} in the near-surface for stations F-L, E4-W, and A3-2 respectively. At the 0.01 % PAR level we observed still significant primary production at F-L, E4-W, and A3-2 stations (0.12, 0.06, and 0.08 µmol C d^{-1} respectively), while at the least productive sites primary production at 0.01 % PAR was low to non-detectable (Fig. 4).

Vertical profiles of NO_3^- assimilation rates closely paralleled the vertical evolution of primary production (Fig. 4) but the decrease in NH_4^+ assimilation with depth was less severe than that for NO_3^-. Nitrate was still preferentially assimilated over ammonium at most of the stations except at the HNLC reference station (Fig. 5a). This resulted in high f ratios, i.e. NO_3^- uptake / (NO_3^- uptake + NH_4^+ uptake) (Dugdale and Goering, 1967), which increased in the euphotic layer from $\sim$ 0.4 at the less productive HNLC reference station to $\sim$ 0.9 at station F-L, north of the polar front.

We observe significant nitrification rates in the mixed layer with maximal rates generally near the bottom of the euphotic layer (Figs. 4 and 5b). Nitrification reached up to $\sim$ 3 µmol N L^{-1} d^{-1}, though $\sim$ 90 % of the values were < 1 µmol N L^{-1} d^{-1} (Fig. 4).

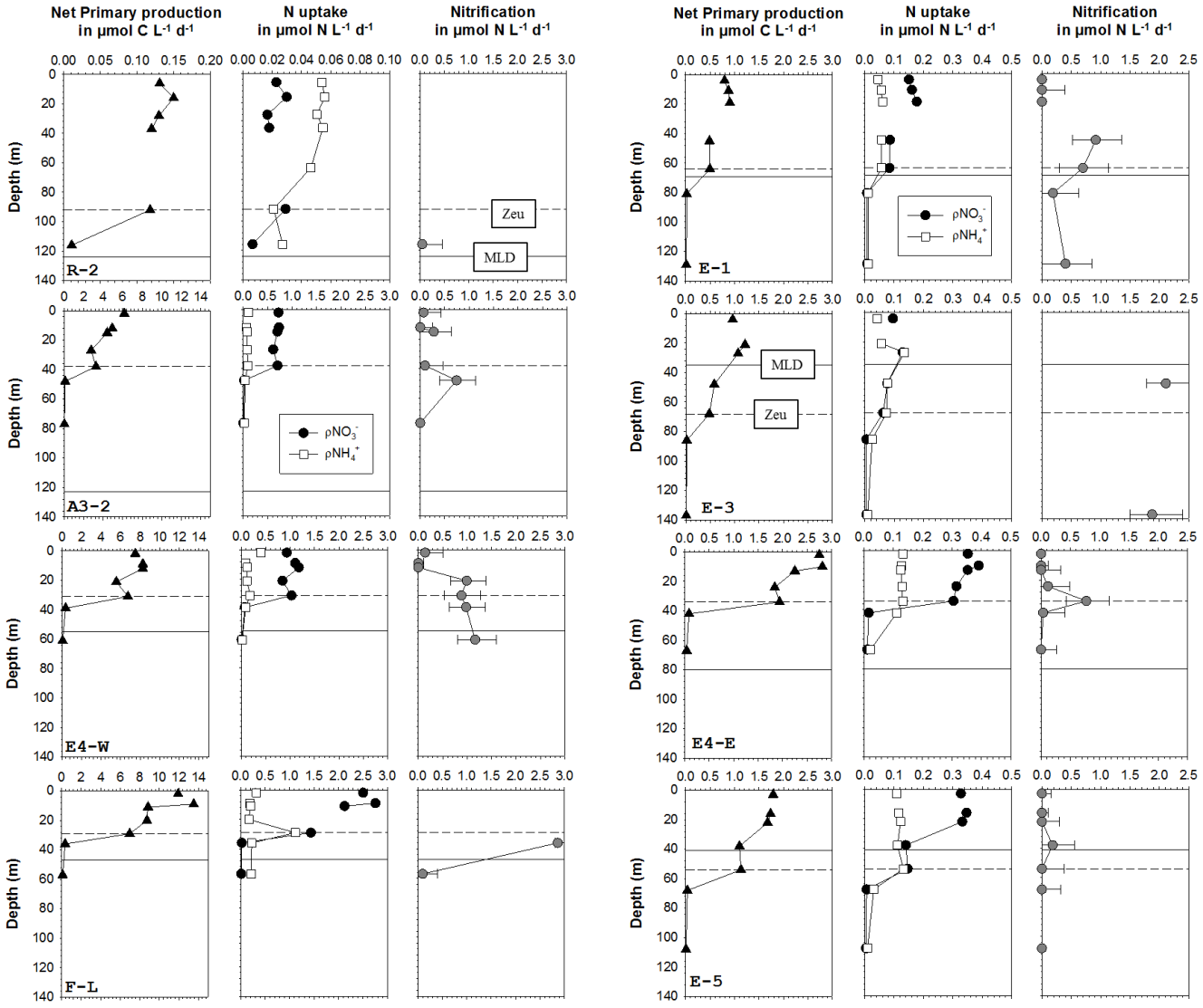

Figure 4. Vertical distribution of net primary production (NPP, left column), N uptake (middle column), and nitrification (right column; error bar corresponding to the 5 and 95 % percentiles) rates between stations (rows). Note that there is a change of scale between reference R-2 site, high productivity sites (A3-2, F-L, E4-W), and meander sites (E1, E3, E4-E, E5). The dashed line represents the euphotic layer depth (Zeu = 1 % PAR attenuation) and the full line represents the mixed layer depth.

4 Discussion

4.1 High primary production in naturally iron-fertilized blooms

Several massive blooms occur in the core of the Antarctic Circumpolar Current in the Kerguelen area (Fig. 1): (i) over the south-eastern Kerguelen Plateau, remarkably constrained by the bathymetry, (ii) in a plume extending eastward through the interaction between the polar front jet, crossing the plateau in a narrow mid-depth channel just to the south of the Kerguelen Island, and the rise bordering the basin to the north, (iii) and to the easternmost part of the study area in a zone of retroflection of the polar front and of eddy mixing between Antarctic and subantarctic surface waters (see Park et al., 2014). This complex distribution is in agreement with an input of iron from the interaction between the iron-deficient Antarctic Circumpolar Current and the local bathymetry (Blain et al., 2007; Sokolov and Rintoul, 2007). Trace metals, and iron in particular, are required for many important cellular processes such as photosynthesis (including photoadaptation), respiration, and nitrate reduction. Iron-enrichment experiments ranging from bottle incubations to large-scale open-ocean amendment studies have demonstrated that iron supply stimulates phytoplankton growth in the Southern Ocean (Martin, 1990; de

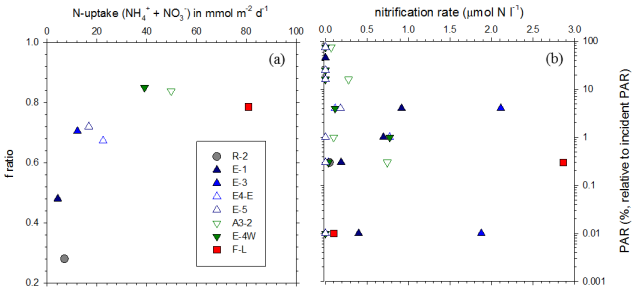

Figure 5. Relationship between mixed layer depth integrated N uptake ($NH_4^+ + NO_3^-$) and f ratio **(a)** and between PAR (%) and nitrification rates **(b)**.

Baar et al., 1990, 2005; Boyd et al., 2007). Primary production up to 130 mmol C m^{-2} d^{-1} has been reported in these iron-fertilized patches (Gall et al., 2001; Gervais et al., 2002; Coale et al., 2004; Smetacek et al., 2012). Naturally iron-fertilized systems usually present higher rates of primary production, e.g. up to ∼ 275 mmol C m^{-2} d^{-1} over the South Georgia plateau (Korb et al., 2005) and up to ∼ 250 mmol C m^{-2} d^{-1} within the fast-flowing, iron-rich jet of the polar front in the Atlantic sector (Jochem et al., 1995) and in the iron-fertilized plume of Crozet Islands (Seeyave et al., 2007). The production rates reported here for the fertilized areas (35 to 315 mmol C m^{-2} d^{-1}) are in line with these previous studies (Table 1), confirming that the spring phytoplankton blooms developing over, and downstream of the Kerguelen Plateau are sustained by very high rates of net primary production. Primary production in the adjacent HNLC area (R-2; ∼ 13 mmol C m^{-2} d^{-1}) is lower and in agreement with the primary production reported for the HNLC pelagic zone in the Southern Ocean (from 4 to 33 mmol C m^{-2} d^{-1}; Arrigo et al., 2008).

At the most productive stations of the different bloom sites, primary production is still occurring below 1 % PAR attenuation, which is generally considered to represent the lower limit of the euphotic layer. Such an observation is not unusual and this has been recently discussed by Marra et al. (2014). In the present study primary production rates generally reach 0 within the confinement of the mixed layer; fluxes were therefore integrated between surface and bottom of the mixed layer. Moreover, the mixed layer is characterized by a steep density gradient at the bottom, implying uniform biogeochemical properties and limited exchanges with the underlying ocean. Primary production, therefore, affects and is affected by the biogeochemical properties of this layer. Note, however, than at stations E-3 and E-5 the euphotic layer extends deeper than the mixed layer, and accordingly there was still some primary production measurable below the mixed layer. Therefore, for these two stations, integration of primary production over the mixed layer underestimates primary production integrated over the euphotic layer by 40 and 20 % respectively.

Notwithstanding the complex interplay between biogeochemical and physical processes in this large-scale natural iron-fertilization experiment, we do observe a strong, relatively simple linear relationship between the amount of biomass (µmol C L^{-1} and µmol N L^{-1}) and both assimilation rates (µmol C L^{-1} d^{-1} and µmol N L^{-1} d^{-1}) and specific growth rates (d^{-1}) (Fig. 3). The increase in biomass normalized primary production with increasing biomass cannot be explained by variations in macronutrient concentrations or temperature in the mixed layer. Indeed, the maximum difference in temperature was less than 2 °C and according to the growth–temperature relationship described in Eppley (1972) such a small range of temperature cannot explain the large change in growth rate. Throughout the study period the uniformly high macronutrient concentrations (Blain et al., 2015; Closset et al., 2014; Fig. 2) remained at levels preventing any Si, P, or N limitation of phytoplankton growth (e.g. Sarthou et al., 2005, and reference therein).

The likeliness of a larger supply of iron and trace metals over the Kerguelen Plateau and north of the polar front (Martin, 1990; de Baar et al., 2005; Boyd et al., 2007; Blain et al., 2007) stands out as the most important cause for the observed differences in primary production (from ∼ 0 to 9 µmol C L^{-1} d^{-1}) and C growth rate (from < 0.1 and 0.3 d^{-1}) between stations (Fig. 3). Over the shallow plateau iron is supplied through the interaction of the bottom waters with sediments and possible igneous outcrops. By this process, subsurface water is becoming enriched in iron, which subsequently can be efficiently supplied to the mixed layer via vertical mixing (Blain et al., 2007; Park et al., 2008). At the polar front, iron fertilization results from the previously described enrichment over the plateau and the spreading of this enrichment eastward through the additional interaction between the polar front jet and local bathymetry (Mongin et al., 2008; Sanial et al., 2015). This mode of supply can be compared with the polar-front-associated bloom in the Atlantic sector, where iron is supplied by lateral advection from the Patagonian shelves and islands in the Scotia Ridge area (de Baar et al., 1995; Löscher et al., 1997) or by direct lithogenic aerosol deposition (Quéguiner et al., 1997). Similar increases in growth rate driven by the degree of iron fertilization (Fig. 3) were reported earlier for the Southern Ocean (e.g. the growth rate increase from < 0.1 to 0.5 d^{-1} in the SOIREE fertilized patch; Gall et al., 2001).

Net primary production during summer over the Kerguelen Plateau (January–February, KEOPS 1; Mosseri et al., 2008; Lefèvre et al., 2008) reached values close to ∼ 80 mmol C m^{-2} d^{-1}. Such rates are lower than those for spring presented here (∼ 200 mmol C m^{-2} d^{-1}) (Table 1). This seasonal pattern is in agreement with satellite Chl-a distribution data showing that the bloom starts in early November, reaches its maximum level in late November–early December, and collapses in January–February (Mongin et al., 2008). Contrasting with the spring situation studied here (KEOPS 2) the summer situation (KEOPS 1) does not show

Table 1. Mixed layer integrated values for particulate organic C (POC), net primary production (NPP), ammonium uptake (NH_4^+ upt.), nitrate uptake (NO_3^- upt.), ammonium + nitrate uptake ($NH_4^+ + NO_3^-$ upt.), nitrification (Nitr.), f ratio, and corrected f ratio by taking into account the contribution of nitrification (Yool et al., 2007).**[**CE]Please explain the bold font used in the table; this should be specified in the caption.

	Date	POC	NPP	NH_4^+ upt.	NO_3^- upt.	$NO_3^- + NH_4^+$ upt.	nitr.*	f ratio	corr. f ratio
		mmol m^{-2}	mmol m^{-2} d^{-1}	mmol m^{-2} d^{-1}	mmol m^{-2} d^{-1}	mmol m^{-2} d^{-1}	mmol m^{-2} d^{-1}	no unit	no unit
HNLC reference station									
R-2	26 Oct 2011	**240.3**	**13.2**	**5.1**	**2.0**	**7.0**		**0.3**	
Meander station									
E-1	30 Oct 2011	436.2	43.5	3.6	8.6	12.2	27.3	0.7	0.0**
E-3	4 Nov 2011	325.8	34.5	2.3	2.1	4.3		0.5	
E4-E	14 Nov 2011	891.0	86.9	7.4	15.2	22.5	8.8	0.7	0.3
E-5	19 Nov 2011	465.4	53.4	4.7	12.1	16.8	2.0	0.7	0.6
Average		**529.6**	**54.6**	**4.5**	**9.5**	**14.0**	**12.7**	**0.6**	**0.3**
SD		**248.3**	**22.9**	**2.2**	**5.6**	**7.7**	**13.1**	**0.1**	**0.3**
Kerguelen Plateau and margin									
E4-W	12 Nov 2011	1276.8	252.8	8.0	41.8	49.8	37.7	0.8	0.1
A3-2	17 Nov 2011	2146.0	179.9	5.9	33.3	39.2	18.1	0.8	0.4
Average		**1711.4**	**216.3**	**7.0**	**37.5**	**44.5**	**27.9**	**0.8**	**0.2**
SD		**614.7**	**51.5**	**1.5**	**6.0**	**7.5**	**13.8**	**0.0**	**0.2**
Polar front									
F-L	7 Nov 2011	**1565.9**	**314.6**	**17.4**	**63.5**	**80.8**		**0.8**	

* Only five stations had a sufficient depth resolution to allow an integration
** As the f ratio is giving the proportion of primary production sustained by new nutrients. If 100 % of the nutrients are considered as regenerated nutrients (nitrification >N uptake), then the proportion of new nutrient is 0.

any relationship between biomass and primary production or growth rate (Fig. 6). In early February (KEOPS 1), primary production and growth rate rapidly decreased in the euphotic layer from about 14 down to 2 µmol C L^{-1} d^{-1} and from ~ 0.3 down to 0.01 d^{-1} respectively. Associated with these changes, the mixed layer production system evolved from being autotrophic, characteristic for spring, to heterotrophic with respiration exceeding photosynthesis (Lefèvre et al., 2008; Christaki et al., 2014). With nitrate and phosphate at non-limiting concentrations, a top-down control of phytoplankton development (mostly diatoms; Georges et al., 2014; Sackett et al., 2014) is the most likely cause of this change during the decay of the bloom in late summer (KEOPS 1; Carlotti et al., 2008; Brussaard et al., 2008; Sarthou et al., 2008). A Si limitation of diatom growth during this period cannot be ruled out either, since measured silicic acid concentrations (~ 1 µmol L^{-1}) are significantly below measured half-saturation constants for Si uptake (5–15 µmol L^{-1}; Mosseri et al., 2008). However, F_v/F_m ratios (ratio of variable fluorescence F_v to the maximum fluorescence F_m, quantitatively related to the efficiency of photochemistry; Falkowski and Raven, 1997) over the plateau in late summer remained high, indicating that the phytoplankton community was relieved from nutrient stress, including iron stress (Timmermans et al., 2008).

To conclude, the resulting increase in integrated primary production (up to 8 times; Table 1) between fertilized (plateau and polar front) and unfertilized areas (HNLC reference site) is similar to the largest increase reported for artificial iron addition experiments worldwide (Boyd et al., 2007; up to 10 times). Despite the much higher primary production for the fertilized area in comparison with the HNLC area, the export of organic matter remains relatively small during spring and summer (Savoye et al., 2008; Planchon et al., 2015). Low export efficiency suggests that the products of primary production are mainly recycled within the mixed layer by an efficient microbial loop (Sarthou et al., 2008; Obernosterer et al., 2008; Christaki et al., 2014; Malits et al., 2014). The carbon sequestration efficiency induced by iron fertilization remains proportionally relatively low (Jacquet et al., 2008, 2015).

4.2 Upper-ocean N cycling: high f ratios and nitrification rates in deep productive mixed layer

Integrated N-uptake rates and f ratios lie in the upper range of values reported for the Southern Ocean (Table 1) and are indicative of a nearly completely NO_3^--based primary production (Sambrotto and Mace, 2000; Savoye et al., 2004; Mulholland and Lomas, 2008; Cochlan, 2008). The f ratio increases with measured N-uptake rates ($NO_3^- + NH_4^+$), from ~ 0.3 in the less-productive HNLC reference station to ~ 0.8 in the productive areas over the Kerguelen Plateau and north of the polar front (Fig. 5a; Table 1). Such a relationship with productivity is in agreement with an enhancement of both specific and absolute NO_3^- uptake rates under iron-replete conditions (Van Leeuwe et al., 1997; Timmermans et al., 1994; Franck et al., 2000; Cochlan et al., 2002; Coale et al., 2004; Lucas et al., 2007) (Fig. 3), as well as with the nat-

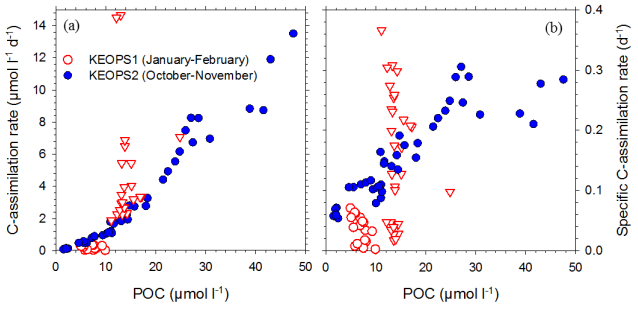

Figure 6. Relationship in the euphotic layer (100 to 1 % PAR) between biomass (POC) and net primary production **(a)** and specific C assimilation rates (growth rate) **(b)**. The KEOPS2 stations are represented in blue, with the circles for the HNLC station (R-2), the normal triangles for the meander stations (E1 to E5), the inverse triangles for the plateau stations (A3-2 and E4-W), and the squares for the station north of the polar front (F-L). The KEOPS1 stations are in red (Raimbault, KEOPS 1 database). Inversed red triangles represent the stations over the south-east Kerguelen Plateau, and the red circles represent the HNLC area east of the plateau (not sampled during KEOPS2).

ural variability of the f ratio in the Southern Ocean related to productivity (HNLC vs. productive areas; Cochlan, 2008). Below the euphotic layer, ammonium is preferentially assimilated over nitrate, with f ratios ranging between 0.1 and 0.5 (data not shown). Assimilation of nitrate is energetically more demanding than assimilation of ammonium and should be more dependent on light. Once nitrate has been transported into the cell, it has to be further reduced into ammonium before it can be assimilated (Mulholland and Lomas, 2008). At the end of summer, the f ratio over the plateau decreases rapidly, from 0.6 to 0.2, indicating that the system evolved from a nitrate-based to an ammonium-based primary production (Mosseri et al., 2008; P. Raimbault, KEOPS 1 database). Such an evolution is in agreement with an increase in ammonium availability in a decaying bloom (Sambrotto and Mace, 2000; Cochlan, 2008). Note that our f ratios are most probably overestimated because they do not take into account the assimilation of dissolved organic nitrogen by phytoplankton (Bronk et al., 2007). However, we note that urea uptake, a proxy for dissolved organic N assimilation, is usually relatively low south of the polar front, where dissolved inorganic N is abundant (Waldron et al., 1995; Sambrotto and Mace, 2000; Savoye et al., 2004).

Nitrification rates are high (up to 3 µmol L^{-1} d^{-1}, with ∼ 90 % of the cases < 1 µmol L^{-1} d^{-1}) at low-light intensities, and insignificant (below our detection limit) at high-light intensities (Figs. 4 and 5b). Such rates (∼ 90 % of the cases) are in the range of maximum rates reported for the open ocean (up to 0.75 µmol L^{-1} d^{-1}) in the Peru Upwelling (Lipschultz et al., 1991; Ward, 2008) and above the one reported for the Southern Ocean (< 0.1 µmol L^{-1} d^{-1}; Olson, 1981; Bianchi et al., 1997). The Southern Ocean nitrification data available in the literature pertain to autumn and winter, seasons during which primary production and remineralization are expected to be low. Nitrification occurs in two steps, the oxidation of ammonium to nitrite and the oxidation of nitrite to nitrate, mediated by distinct groups of microorganisms (Ward, 2008). We only assessed the second step of the nitrification processes (i.e. nitrate production). However, a balance between the first and second steps is likely, given the relatively low and constant ammonium and nitrite concentrations in the mixed layer (Fig. 2) even at the seasonal scale (Fripiat et al., 2015).

The observed variation of nitrification with depth supports the fact that the process is partly light inhibited (Fig. 5b) and this is in agreement with what we know about the distribution of nitrification in the ocean (Hagopian and Riley, 1998; Ward, 2008). High nitrification rates are usually reported near the bottom of the euphotic layer where organic matter is still abundant and light is much reduced, allowing the nitrifiers to compete with phytoplankton for the ammonium produced by remineralization (Lipschultz et al., 1991; Ward, 2008). Below the euphotic layer, organic matter degradation and organic matter export lead to ammonium release which is in fine transformed into nitrate (Ward and Zafiriou, 1988; Newel et al., 2011). As the process closing the internal N cycle ($NO_3^- \rightarrow$ PON $\rightarrow NO_3^-$) nitrification likely tracks primary production. The unusual high rates of nitrification across the study area likely result from the particularly high rates of primary production, which are in the upper range for those observed in the Southern Ocean (Sect. 4.1).

The particularity of our study is that a significant fraction of the mixed layer (except for stations E-3 and E-5) extends below the euphotic layer (Fig. 4). The nitrate produced by nitrification at low-light intensities can be easily transported into the euphotic layer and supports directly regenerated primary production. Such findings have profound consequences on the concept of new production (Dudgale and Goering, 1967; Eppley and Petterson, 1979). Under steady-state conditions and averaged over appropriate timescales, new production is the fraction of primary production that can be exported from the euphotic layer, without depleting the system in nutrients. New production is therefore balanced by the supply of new nutrients into the euphotic layer. New nutrients are distantly produced, supplied into the euphotic layer by water mixing or atmospheric deposition/exchange, and assimilated during the vegetative season. Generally in the ocean, the euphotic layer is deeper than the mixed layer (e.g. in the low-latitude oceans). Under such conditions, nitrate produced by nitrification below the euphotic layer can only become available for subsequent primary production by diapycnal mixing, through the lower boundary of the mixed layer. In this context, nitrate has generally been considered as a new nutrient (Dugdale and Goring, 1967), especially in the Southern Ocean where it is also considered to be the dominant nitrogen source assuming negligible N_2 fixation. Following this rationale, new production in the Southern Ocean

is usually calculated by multiplying the primary production with the f ratio (Eppley and Peterson, 1979; Savoye et al., 2004). However, nitrification in a deep mixed layer may fuel an important input of nitrate in the euphotic layer with, therefore, a significant fraction of nitrate-based primary production being actually regenerated production. To calculate correctly the new production (f ratio $\times$ NPP), one needs to subtract the nitrification term from the nitrate uptake term (Yool et al., 2007). The nitrification depth profiles were well resolved at only five stations, permitting nitrification rates to be integrated over the mixed layer depth (Table 1). For the productive stations A3-2 and E4-W where low light (< 1 % PAR) prevails over 40–70 % of the mixed layer, nitrification decreased the f ratio from $\sim 0.8 \pm 0.0$ to $\sim 0.2 \pm 0.2$, implying that 70 ± 30 % of the nitrate uptake was sustained by nitrification. This is in agreement with Fripiat et al. (2015), who simulated the change of the fixed N pools and their isotopic composition (δ^{15}N and δ^{18}O) from October to February for the Kerguelen Plateau and show that nitrification can account for 40 to 80 % of the seasonal nitrate assimilation. The significance of nitrification above the plateau was also inferred from the temporal change of the nitrate isotopic composition during spring (KEOPS 2), sustaining ~ 50 % of the nitrate assimilation (Dehairs et al., 2015). By inspecting the short-term changes in the meander area, the contribution of nitrification to nitrate assimilation varies significantly between successive visits. During the first visit in the meander area (E-1), integrated nitrification was higher than that of integrated nitrate uptake. This implies that 100 % of the nitrate assimilated by phytoplankton originates from regeneration. This contribution decreases during the two subsequent visits, implying the f ratio to change from 0.7 to 0.3 and from 0.7 to 0.6 for E4-E and E-5 respectively. The low contribution of nitrification during the last visit is in agreement with a mixed layer depth (MLD) being shallower than the euphotic layer depth, implying a vertical segregation between nitrate uptake and nitrification delimitated by a sharp density gradient defining the MLD.

High mixed layer nitrification rates in the fertilized area are also in agreement with (i) the measured low carbon export efficiency (NPP / ^{234}Th-export, with ^{234}Th-export estimated at 100 m; Planchon et al., 2015) and (ii) the low seasonal nitrate depletion (Mosseri et al., 2008) despite high nitrate assimilation rates in the mixed layer. Significant nitrification can also explain why silicic acid is depleted (with high biogenic silica production : dissolution ratio) but not nitrate (Mosseri et al., 2008; Closset et al., 2014). $Si : NO_3$ assimilation ratios were close to 1 (Mosseri et al., 2008; Closset et al., 2014), in accordance with what is expected for non-limiting iron conditions (Takeda, 1998; Hutchins and Bruland, 1998). Without nitrification, nitrate should be depleted similar to silicic acid. The hypothesis put forward by Mosseri et al. (2008) attributes this peculiar decoupling to the capacity of diatoms to grow on ammonium resulting from high heterotrophic activity. Such a hypothesis appears unlikely here since for all stations, except R-2, ammonium assimilation rates are much lower than nitrate assimilation rates. Thus, we hypothesize that in a deep mixing system nitrifiers can efficiently compete with phytoplankton for ammonium.

5 Conclusions

This study confirms the impact of iron fertilization on primary production in the Southern Ocean. Naturally fertilized areas sustain a much higher integrated primary production (up to 315 mmol C m^{-2} d^{-1}) and growth rates (up to 0.31 d^{-1}) than unfertilized HNLC areas (12 mmol C m^{-2} d^{-1}; 0.06 d^{-1} respectively). Primary production in the euphotic layer of the fertilized areas is mainly sustained by nitrate uptake (f ratio up to 0.9). In the unfertilized areas, the contribution of ammonium to primary production increases. However, part of the nitrate assimilation by phytoplankton is provided from mixed layer nitrification which is high (up to ~ 3 µmol N L^{-1} d^{-1}, with ~ 90 % of them < 1 µmol N L^{-1} d^{-1}) and presents maximum rates at the base of the euphotic zone and below. Such high nitrification rates can be explained by (i) a deep mixed layer – encompassing the euphotic layer – allowing nitrate assimilation and regeneration to take place within the same water mass and (ii) the especially high rates of primary production making the studied Kerguelen area one of the most productive systems in the open ocean, likely stimulating nitrogen N assimilation and regeneration. All these conditions likely contribute to creating a favourable environment for nitrifiers.

The Supplement related to this article is available online at doi:10.5194/bg-12-6515-2015-supplement.

Acknowledgements. Our warm thanks go to the captain, officers, and crew of the R/V *Marion Dufresne* for their support during the KEOPS 2 field work. This research was supported by the Federal Belgian Science Policy Office (BELSPO), Science for Sustainable Development (SSD) program (contract SD/CA/05A); Flanders Research Foundation (FWO grant G071512N); and VUB Strategic Research Plan. François Fripiat is a post-doctoral fellow with the Flanders Research Foundation (FWO, Belgium). Camila Fernandez was partially funded by Fondap 15110027. Lennin Florez-Leiva received support from the LIA MORFUN project. The KEOPS 2 project was supported by the French research program of INSU-CNRS LEFE-CYBER ("Les enveloppes fluides et l'environnement" – "Cycles biogéochimiques, environnement et ressources"), the French ANR ("Agence Nationale de la Recherche", SIMI-6 program), the French CNES ("Centre National d'Etudes Spatiales"), and the French Polar Institute IPEV (Institut Polaire Paul-Emile Victor). The altimeter and colour/temperature products for the Kerguelen area were produced by Ssalto/Duacs and CLS with support from CNES.

Edited by: I. Obernosterer

References

Aminot, A. and Kérouel, R.: Dosage automatique des nutriments dans les eaux marines: methods en flux continu, Ed. Ifremer, 2007.

Arrigo, K. R., van Dijken, G. L., and Bushinsky, S.: Primary production in the Southern Ocean, 1997–2006, J. Geophys. Res., 113, C08004, doi:10.1029/2007JC004551, 2008.

Bianchi, M., Feliatra, F., Tréguer, P., Vincedeau, M.-A., and Morvan, J.: Nitrification rates, ammonium and nitrate distribution in upper layers of the water column and in sediments of the Indian sector of the Southern Ocean, Deep-Sea Res. Part II, 44, 1017–1032, 1997.

Blackburn, T. H.: A method for measuring rates of NH_4^+ turnover in anoxic marine sediments using a ^{15}N-NH_4^+ dilution technique, Appl. Environ. Microbiol., 37, 760–765, 1979.

Blain, S., Tréguer, P., Belviso, S., Bucciarelli, E., Denis, M., Desabre, S., Fiala, M., Jezequel, V. M., Lefevre, J., Mayzaud, M., Marty, J.-C., and Razouls, S.: A biogeochemical study of the island mass effect in the context of the iron hypothesis : Kerguelen Islands, Southern Ocean, Deep-Sea Res. Part I, 48, 163–187, 2001.

Blain, S., Quéguiner, B, Armand, L., Belviso, S., Bombled, B.,Bopp, L., Bowie, A., Brunet, C., Brussaard, C., Carlotti, F., Christaki, U., Corbière, A., Durand, I., Ebersbach, F., Fuda, J.-L., Garcia, N., Gerringa, L., Griffiths, B., Guigue, C., Guillerm, C., Jacquet, S., Jeandel, C., Laan, P., Lefèvre, D., Lo Monaco, C., Malits, A., Mosseri, J., Obernosterer, I., Park, Y.-H., Picheral, M., Pondaven, P., Remenyi, T., Sandroni, V., Sarthou, G., Savoye, N., Scouarnec, L., Souhaut, M., Thuiller, D., Timmermans, K., Trull, T., Uitz, J., van Beek, P., Veldhuis, M., Vincent, D., Viollier, E., Vong, L., and Wagener, T.: Effect of natural iron fertilization on carbon sequestration in the Southern Ocean, Nature, 446, 1070–1074, doi:10.1038/nature05700, 2007.

Blain, S., Quéguiner, B., and Trull, T. W.: The natural iron fertilization experiment KEOPS (KErguelen Ocean and Plateau compared Study): an overview, Deep-Sea Res. Part II, 55, 559–565, 2008.

Blain, S., Capparos, J., Guéneuguès, A., Obernosterer, I., and Oriol, L.: Distributions and stoichiometry of dissolved nitrogen and phosphorus in the iron-fertilized region near Kerguelen (Southern Ocean), Biogeosciences, 12, 623–635, doi:10.5194/bg-12-623-2015, 2015.

Bowie, A., Trull, T. W., and Dehairs, F.: Estimating the sensitivity of the subantarctic zone to environmental change: the SAZ-Sense project, Deep-Sea Res. Part II, 58, 2051–2058, 2011.

Boyd, P. W., Jickells, T., Law, C. S., Blain, S., Boyle, E. A., Buesseler, K. O., Coale, K. H., Cullen, J. J., de Baar, H. J. W., Follows, M., Harvey, M., Lancelot, C., Levasseur, M., Owens, N. P. J., Pollard, R., Rivkin, R. B., Sarmiento, J., Schoemann, V., Smetacek, V., Takeda, S., Tsuda, A., Turner, S., and Watson, A. J.: Mesoscale Iron Enrichment Experiments 1993–2005: Synthesis and future directions, Science, 315, 612, doi:10.1126/science.1131669, 2007.

Bronk, D. A., Glibert, P. M., and Ward, B. B.: Nitrogen uptake, dissolved organic nitrogen release, and new production, Science, 265, 1843–1846, 1994.

Bronk, D. A., See, J. H., Bradley, P., and Killberg, L.: DON as a source of bioavailable nitrogen for phytoplankton, Biogeosciences, 4, 283–296, doi:10.5194/bg-4-283-2007, 2007.

Brussaard, C. P. D., Timmermans, K. R., Uitz, J., and Veldhuis, M. J. W.: Virioplankton dynamics and virally induce phytoplankton lysis versus microzooplankton grazing southeast of the Kerguelen (Southern Ocean), Deep-Sea Res. Part II, 55, 752–765, 2008.

Carlotti, F., Thibault-Botha, D., Nowaczyk, A., and Lefèvre, D.: Zooplankton community structure, biomass and role in carbon fluxes during the second half of a phytoplankton bloom in the eastern sector of the Kerguelen shelf (January–February 2005), Deep-Sea Res. Part II, 55, 720–733, 2008.

Christaki, U., Lefèvre, D., Georges, C., Colombet, J., Catala, P., Courties, C., Sime-Ngando, T., Blain, S., and Obernosterer, I.: Microbial food web dynamics during spring phytoplankton blooms in the naturally iron-fertilized Kerguelen area (Southern Ocean), Biogeosciences, 11, 6739–6753, doi:10.5194/bg-11-6739-2014, 2014.

Closset, I., Lasbleiz, M., Leblanc, K., Quéguiner, B., Cavagna, A.-J., Elskens, M., Navez, J., and Cardinal, D.: Seasonal evolution of net and regenerated silica production around a natural Fe-fertilized area in the Southern Ocean estimated with Si isotopic approaches, Biogeosciences, 11, 5827–5846, doi:10.5194/bg-11-5827-2014, 2014.

Cochlan, W. P.: Nitrogen Uptake in the Southern Ocean, in: Nitrogen in the Marine Environment, edited by: Capone, D. G., Bronk, D. A., Mulholland, M. R., and Carpenter, E. J., 2nd Edition, Academic Press, Elsevier, 569–596, 2008.

Cochlan, W. P., Bronk, D. A., and Coale, K. H.: Trace metals and nitrogenous nutrition of Antarctic phytoplankton: experimental observations in the Ross Sea, Deep-Sea Res. II, 49, 3365–3390, 2002.

Coale, K. H., Johnson, K. S., Chavez, F. P., Buesseler, K. O., Barber, R. T., Brzezinski, M. A., Cochlan, W. P., Millero, F. J., Falkowski, P. G., Bauer, J. E., Wanninkhof, R. H., Kudela, R. M., Altabet, M. A., Hales, B. E., Takahashi, T., Landry, M. R., Bidigare, R. R., Wang, X., Chase, Z., Strutton, P. G., Friederich, G. E., Gorbunov, M. Y., Lance, V. P., Hilting, A. K., Hiscock, M. R., Demarest, M., Hiscock, W. T., Sullian, K. F., Tanner, S. J., Gordon, R. M., Hunter, C. N., Elrod, V. A., Titzwater, S. E., Jones, J. L., Tozzi, S., Koblizek, M., Roberts, A. E., Herndon, J., Brewster, J., Ladizinsky, N., Smith, G., Cooper, D., Timothy, D., Brown, S., Selph, K. E., Sheridan, C. C., Twining, B. S., and Johnson, Z. I.: Southern Ocean Iron Enrichment Experiment: carbon cycling in high- and low-Si waters, Science, 304, 408–414, doi:10.1126/science.1089778, 2004.

de Baar, H. J. W., Buma, A. G. J., Nolting, R. F., Cadee, G. C., Jacques, G., and Treguer, P. J.: On iron limitation of the Southern Ocean: experimental observations in the Weddell and Scotia Seas, Mar. Ecol. Prog. Ser., 65, 105–122, 1990.

de Baar, H. J. W., de Jong, J. T. M., Bakker, D. C. E., Löscher, B. M., Veth, C., Bathmann, U., and Smetacek, V.: Importance of iron for plankton blooms and carbon dioxide drawdown in the Southern Ocean, Nature, 373, 412–415, 1995.

de Baar, H. J. W., Boyd, P. W., Coale, K. H., Landry, M. R., Tsuda, A., Assmy, P., Bakker, D. C. E., Bozec, Y., Barber, R. T., Brzezinski, M. A., Buesseler, K. O., Boyé, M., Croot, P. L., Gervais, F., Gorbunov, M. Y., Harrison, P. J., Hiscock, W. T., Laan, P., Lancelot, C., Law, C. S., Levasseur, M., Marchetti,

A., Millero, F., Nishioka, J., Nojiro, Y., van Oijen, T., Riebesell, U., Rijkenberg, M. J. A., Saito, H., Takeda, S., Timmermans, K. R., Veldhuis, M. J. W., Waite, A. M., and Wong, C.-S.: Synthesis of iron fertilization experiments: from the iron age in the age of enlightenment, J. Geophys. Res., 110, C09S16, doi:10.1029/2004JC002601, 2005.

de Boyer Montégut, C., Madec, G., Fischer, A. S., Lazar, A., and Iudicione, D.: Mixed layer depth over the global ocean: an examination of profile data and a profile-based climatology, J. Geophys. Res., 109, C12003, doi:10.1029/2004JC002378, 2004.

Dehairs, F., Fripiat, F., Cavagna, A.-J., Trull, T. W., Fernandez, C., Davies, D., Roukaerts, A., Fonseca Batista, D., Planchon, F., and Elskens, M.: Nitrogen cycling in the Southern Ocean Kerguelen Plateau area: evidence for significant surface nitrification from nitrate isotopic compositions, Biogeosciences, 12, 1459–1482, doi:10.5194/bg-12-1459-2015, 2015.

Doty, M. S. and Oguri, M.: The island mass effect, Journal of International Council for Exploration of Sea, 22, 33–37, 1956.

Dugdale, R. C. and Goering, J. J.: uptake of new and regenerated form of nitrogen in primary productivity, Limnol. Oceanogr., 12, 196–206, 1967.

Elskens, M., Baeyens, W., and Goeyens, L.: Contribution of nitrate to the uptake of nitrogen by phytoplankton in an ocean margin environment, Hydrobiologia, 353, 139–152, 1997.

Elskens, M., Baeyens, W., Brion, N. N., De Galan, S., Goeyens, L., and de Brauwere, A.: Reliability of N flux rates estimated from ^{15}N enrichment and dilution experiments in aquatic systems, Global Biogeochem. Cy., 19, GB4028, doi:10.1029/2004GB002332, 2005.

Eppley, R. W.: Temperature and phytoplankton growth in the sea, Fishery Bulletin, 70, 1063–1085, 1972.

Eppley, R. W. and Peterson, B. J.: Particulate organic matter flux and planktonic new production in the deep ocean, Nature, 282, 677–680, 1979.

Falkowski, P. G. and Raven, J. A.: The efficiency of photochemistry *in* Chapter 3 The photosynthetic light reactions, p. 92 in Aquatic Photosynthesis, eds. Blackwell Science, 375 pp., 1997.

Falkowski, P. G., Barber, R. T., and Smetacek, V.: Biogeochemical controls and feedbacks on ocean primary production, Science, 281, 200–206, 1998.

Franck, V. M., Brzezinski, M. A., Coale, K. H., and Nelson, D. M.: Iron and silicic acid concentrations regulate Si uptake north and south of the Polar Frontal Zone in the Pacific sector of the Southern Ocean, Deep-Sea Res. Part 2, 47, 3315–3338, 2000.

Fripiat, F., Elskens, M., Trull, T.W., Blain, S., Cavagna, A.-J., Fernandez, C., Fonseca-Batista, D., Planchon, F., Raimbault, P., Roukaert, A., and Dehairs, F.: Significant mixed layer nitrification in a natural iron-fertilized bloom of the Southern Ocean, in review, Global Biogeochem. Cy., in press, 2015.

Gall, M. P., Strzepek, R., Maldonado, M., and Boyd, P.: Phytoplankton processes. Part 2: Rates of primary production and factors controlling algal growth during the Southern Ocean Iron Release Experiment (SOIREE), Deep-Sea Res. Part II, 48, 2571–2590, 2001.

Gervais, F., Riebesell, U., and Gorbunov, M. Y.: Changes in Primary Productivity and Chlorophyll a in response to iron fertilization in the Southern Polar frontal zone, Limnol. Oceanogr., 47, 1324–1335, 2002.

Georges, C., Monchy, S., Genitsaris, S., and Christaki, U.: Protist community composition during early phytoplankton blooms in the naturally iron-fertilized Kerguelen area (Southern Ocean), Biogeosciences, 11, 5847–5863, doi:10.5194/bg-11-5847-2014, 2014.

Gille, S. T., Carranza, M. M., Cambra, R., and Morrow, R.: Wind-induced upwelling in the Kerguelen Plateau region, Biogeosciences, 11, 6389–6400, doi:10.5194/bg-11-6389-2014, 2014.

Glibert, P. M., Lipschultz, F., McCarthy, J. J., and Altabet, M. A.: Isotope dilution models of uptake and remineralization of ammonium by marine plankton, Limnol. Oceanogr., 27, 639–650, 1982.

Hagopian, D. S. and Riley, J. G.: A closer look at the bacteriology of nitrification, Aquacultural Engineering, 19, 223–244, 1998.

Heywood, K. J., Barton, E. D., and Simpson, J. H.: The effects of flow disturbance by an oceanic island, J. Mar. Res., 48, 55–73, 1990.

Holmes, R. H., Aminot, A., Kérouel, R., Hooker, B. A., and Peterson, B. J.: A simple and precise method for measuring ammonium in marine and freshwater ecosystems, Can. Fish. Aquat. Sci., 56, 1801–1808, 1999.

Hutchins, D. A. and Bruland, K. W.: Iron-limited diatom growth and Si:N uptake ratios in a coastal upwelling regime, Nature, 393, 561–564, doi:10.1038/31203, 1998.

Jochem, F. J., Mathot, S., and Quéguiner, B.: Size-fractionated primary production in the open Southern Ocean in austral spring, Polar Biol., 15, 381–392, 1995.

Jacquet, S. H. M., Dehairs, F., Savoye, N., Obernosterer, I., Christaki, U., Monnin, C., and Cardinal, D.: Mesopelagic organic carbon remineralization in the Kerguelen Plateau region tracked by biogenic particulate Ba, Deep-Sea Res. Part 2, 868–879, 2008.

Jacquet, S. H. M., Dehairs, F., Lefèvre, D., Cavagna, A. J., Planchon, F., Christaki, U., Monin, L., André, L., Closset, I., and Cardinal, D.: Early spring mesopelagic carbon remineralization and transfer efficiency in the naturally iron-fertilized Kerguelen area, Biogeosciences, 12, 1713–1731, doi:10.5194/bg-12-1713-2015, 2015.

Korb, R. E., Whitehouse, M. J., Thorpe, S. E., and Gordon, M.: Primary production across the Scotia Sea in relation to the physicochemical environment, J. Mar. Sys., 57, 231–249, 2005.

Laws, E., Sakshaug, E., Babin, M., Dandonneau, Y., Falkowski, P., Geider, R., Legendre, L., Morel, A., Sondergaard, M., Takahashi, M., and Williams, P. J.: Photosynthesis and Primary productivity in marine ecosystems: Practical aspects and application of techniques, Joint Global Ocean Flux Study – JGOFS – Report No. 36, 2002.

Lefèvre, D., Guigue, C., and Obernosterer, I.: The metabolic balance at two contrasting sites in the Southern Ocean: The iron fertilized Kerguelen area and HNLC waters, Deep Sea Res. Part 2, 766–776, 2008.

Le Quéré, C., Rödenbeck, C., Buithenhuis, E. T., Conway, T. J., Langenfelds, R., Gomez, A., Labuschagne, C., Ramonet, M., Nakazawa, T., Metzl, N., Gillett, N., and Heinmann, M.: Saturation of Southern Ocean CO_2 sink due To recent climate change, Science, 316, 1735, doi:10.1126/science.1136188, 2007.

Lipschultz, F., Wofsy, S. C., Ward, B. B., Codispoti, L. A., Friedrich, G., and Elkins, J. W.: Bacterial transformations of inorganic nitrogen in the oxygen-deficient waters of the Eastern

Tropical South Pacific Ocean, Deep-Sea Res. Part II, 37, 1513–1541, 1991.

Löscher, B. M., de Jong, J. T. M., de Baar, H. J. W., Veth, C., and Dehairs, F.: The distribution of Fe in the Antarctic Circumpolar Current, Deep Sea Res. Part II, 44, 143–188, 1997.

Lucas, M. I., Seeyave, S., Sanders, R., Moore, C. M., Williamson, R., and Stinchcombe, M.: Nitrogen uptake responses to a naturally iron-fertilized phytoplankton bloom during the 2004/2005 CROZEX study, Deep-Sea Res. Part 2, 54, 2138–2173, 2007.

Malits, A., Christaki, U., Obernosterer, I., and Weinbauer, M. G.: Enhanced viral production and virus-mediated mortality of bacterioplankton in a natural iron-fertilized bloom event above the Kerguelen Plateau, Biogeosciences, 11, 6841–6853, doi:10.5194/bg-11-6841-2014, 2014.

Marra, J. F., Lance, V. P., Vaillancourt, R. D., and Hargreaves, B. R.: Resolving the ocean's euphotic zone, Deep Sea Res. Part I, 83, 45–50, 2014.

Martin, J. H.: Glacial interglacial CO_2 change: the iron hypothesis, Paleoceanography, 5, 1–13, 1990.

Mongin, M., Molina, E., and Trull, T. W.: Seasonality and scale of the Kerguelen plateau phytoplankton bloom: A remote sensing and modeling analysis of the influence of natural iron fertilization in the Southern Ocean, Deep-Sea Res. Part II, 55, 880–892, 2008.

Mosseri, J., Quéguiner, B., Armand, L., and Cornet-Barthaux, V.: Impact of iron on silicon utilization by diatoms in the Southern Ocean: a case study of Si/N cycle decoupling in a naturally iron enriched area, Deep-Sea Res. Part II, 55, 801–819, 2008.

Mulholland, M. R. and Lomas, M. W.: N-uptake and assimilation, in: Nitrogen in the Marine Environment, edited by: Capone, D. G., Bronk, D. A., Mulholland, M. R., and Carpenter, E. J., 303—384, Elsevier/Academic, 2008.

Nelson, D. M. and Goering, J. J.: A stable isotope tracer method to measure silicic acid uptake by marine phytoplankton, Anal. Biogeochem., 78, 139–147, 1977a.

Nelson, D. M. and Goering, J. J.: Near surface silica dissolution in the upwelling region off northwest Africa, Deep Sea Res., 24, 65–73, 1977b.

Newel, S. E., Babbin, A. R., Jayakumar, A., and Ward, B. B.: Ammonia oxidation rates and nitrification in the Arabian Sea, Global Biogeochem. Cy., 25, GB4016, doi:10.1029/2010GB003940, 2011.

Obernosterer, I., Christaki, U., Lefèvre, D., Catala, P., Van Wambeke, F., and Lebaron, P.: Rapid bacterial mineralization of organic carbon produced during a phytoplankton bloom induced by natural iron fertilization in the Southern Ocean, Deep-Sea Res. Part II, 55, 777–789, doi:10.1016/j.dsr2.2007.12.005, 2008.

Olson, R. J.: ^{15}N tracer studies of the primary nitrite maximum, J. Mar. Res., 39, 203–238, 1981.

Park, Y.-H., Roquet, F., Durand, I., and Fuda, J.-L.: Large-scale circulation over and around the Northern Kerguelen Plateau, Deep-Sea Res. Part II, 55, 566–581, 2008.

Park, Y.-H., Durand, I., Kestenare, E., Rougier, G., Zhou, M., d'Ovidio, F., Cotté, C., and Lee, J. H.: Polar Front around the Kerguelen Islands: an up-to-date determination and associated circulation of surface/subsurface waters, J. Geophys. Res.-Oceans, 119, 6575–6592, doi:10.1002/2014JC010061, 2014.

Planchon, F., Ballas, D., Cavagna, A.-J., Bowie, A. R., Davies, D., Trull, T., Laurenceau-Cornec, E. C., Van Der Merwe, P., and Dehairs, F.: Carbon export in the naturally iron-fertilized Kerguelen area of the Southern Ocean based on the ^{234}Th approach, Biogeosciences, 12, 3831–3848, doi:10.5194/bg-12-3831-2015, 2015.

Pollard, R., Sanders, R., Lucas, M., and Statham, P.: The Crozet natural iron bloom and export experiment (CROZEX), Deep-Sea Res. Part II, 54, 1905–1914, doi:10.1016/j.dsr2.2007.07.023, 2007.

Pollard, R. T., Slater, I., Sanders, R. J., Lucas, M. I., Moore, C. M., Mills, R. A., Statham, P. J., Allen, J. T., Baker, A. R., Bakker, D. C. E., Charette, M. A., Fielding, S., Fones, G. R., French, M., Hickman, A. E., Holland, R. J., Hughes, J. A., Jickells, T. D., Lampitt, R. S., Morris, P. J., Nédélec, F. H., Nielsdottir, M., Planquette, H., Popova, E. E., Poulton, A. J., Read, J. F., Seeyave, S., Smith, T., Stinchcombe, M., Taylor, S., Thomalla, S., Venables, H. J., Williamson, R., and Zubkov, M. V.: Southern Ocean deep-water carbon export enhanced by natural iron fertilization, Nature, 457, 577–580, doi:10.1038/nature07716, 2009.

Quéguiner, B., Tréguer, P., Peeken, I., and Sharek, R.: Biogeochemical dynamics and the silicon cycle in the Atlantic sector of the Southern Ocean during austral spring 1992, Deep-Sea Res. Part II, 69–89, 1997.

Quéguiner, B.: Iron fertilization and the structure of planktonic communities in high nutrient regions of the Southern Ocean, Deep-Sea Res. Part II, 90, 43–54, doi:10.1016/j.dsr2.2012.07.024, 2013.

Rees, A. P., Owens, N. J. P., Heath, M. R., Plummer, D. H., and Bellerby, R. S.: Seasonal nitrogen assimilation and carbon fixation in a fjordic sea loch, J. Plankton Res., 17, 1307–1324, 1995.

Sackett, O., Armand, L., Beardall, J., Hill, R., Doblin, M., Connelly, C., Howes, J., Stuart, B., Ralph, P., and Heraud, P.: Taxon-specific responses of Southern Ocean diatoms to Fe enrichment revealed by synchrotron radiation FTIR microspectroscopy, Biogeosciences, 11, 5795–5808, doi:10.5194/bg-11-5795-2014, 2014.

Sambrotto, R. N. and Mace, B. J.: Coupling of biological and physical regimes across the Antarctic Polar Front as reflected by nitrogen production and recycling, Deep-Sea Res. Part II, 47, 3339–3367, 2000.

Sanial, V., van Beek, P., Lansard, B., Souhaut, M., Kestenare, E., d'Ovidio, F., Zhou, M., and Blain, S.: Use of Ra isotopes to deduce rapid transfer of sediment-derived inputs off Kerguelen, Biogeosciences, 12, 1415–1430, doi:10.5194/bg-12-1415-2015, 2015.

Sarmiento, J. L., Gruber, N., Brzezinski, M. A., and Dunne, J. P.: High-latitude controls of thermocline nutrients and low latitude biological productivity, Nature, 427, 56–60, 2004.

Sarthou, G., Timmermans, K. R., Blain, S., and Tréguer, P.: Growth physiology and fate of diatoms in the oceans: a review, J. Sea Res., 53, 25–42, 2005.

Sarthou, G., Vincent, D., Christaki, U., Obernosterer, I., Timmermans, K. R., and Brussaard, C. P. D.: The fate of biogenic iron during phytoplankton bloom induced by natural fertilization: Impact of copepod grazing, Deep-Sea Res. Part II, 55, 734–751, 2008.

Savoye, N., Dehairs, F., Elskens, M., Cardinal, D., Kopczynska, E. E., Trull, T. W., Wright, S., Baeyens, W., and Griffiths,

B. F.: Regional variation of spring N-uptake and new production in the Southern Ocean, Geophys. Res. Lett., 31, L03301, doi:10.1029/2003GL018946, 2004.

Savoye, N., Trull, T. W., Jacquet, S. H. M., Navez, J., and Dehairs, F.: ^{234}Th-based export fluxes during a natural iron fertilization experiment in the Southern Ocean (KEOPS), Deep-Sea Res. Part II, 55, 841–855, 2008.

Seeyave, S., Lucas, M. I., Moore, C. M., and Poulton, A. J.: Phytoplankton productivity and community structure across the Crozet Plateau during summer 2004/2005, Deep-Sea Res. Part II, 54, 2020–2044, doi:10.1016/j.dsr2.2007.06.010, 2007.

Sigman, D. M., Altabet, M. A., McCorkle, D. C., Francois, R., and Fischer, G.: The δ^{15}N of nitrate in the Southern Ocean: Consumption of nitrate in surface waters, Global Biogeochem. Cy., 13, 1149–1166, 1999.

Sigman, D. M., Casciotti, K. L., Andreani, M., Barford, C., Galanter, M., and Böhlke, J. K.: A bacterial method for the nitrogen isotopic analysis of nitrate in seawater and freshwater, Anal. Chem., 73, 4145–4153, 2001.

Slawyk, G., Coste, B., Collos, Y., and Rodier, M.: Isotopic and enzymatic analyses of planktonic nitrogen in the vicinity of Cape Sines (Portugal) during weak upwelling activity, Deep-Sea Res. Part I, 44, 1–25, 1997.

Smetacek, V., Klaas, C., Strass, V. H., Assmy, P., Montresor, M., Cisewski, B., Savoye, N., Webb, A., d'Ovidio, F., Arrieta, J. M., Bathmann, U., Bellerby, R., Berg, G. M., Croot, P., Gonzalez, S., Henjes, J., Herndl, G. J., Hoffmann, L. J., Leach, H., Losch, M., Mills, M. M., Neill, C.,Peeken, I., Röttgers, R., Sachs, O., Sauter, E., Schmidt, M. M., Schwartz, J., Terbrüggen, A., and Wolf-Gladrow, D.: Deep carbon export from a Southern Ocean iron-fertilized diatom bloom, Nature, 487, 313–319, doi:10.1038/nature11229, 2012.

Sokolov, S. and Rintoul, S. R.: On the relationship between fronts of the Antarctic Circumpolar Current and surface chlorophyll concentration in the Southern Ocean, J. Geophys. Res., 112, C07030, doi:10.1029/2006JC004072, 2007.

Takahashi, T., Sutherland, S. C., Wanninkhof, R., Sweeney, C., Feely, R. A., Chipman, D. W., Hales, B., Friederich, G., Chavez, F., Sabine, C., Watson, A., Bakker, D. C. E., Schuster, U., Metzl, N., Yoshikawa-Inoue, H., Ishii, M., Midorikawa, T., Nojiri, Y., Körtzinger, A., Steinhoff, T., Hoppema, M., Olafsson, J., Arnarson, T. S., Tilbrook, B., Johannessen, T., Olsen, A., Bellerby, R., Wong, C. S., Delille, B., Bates, N. R., and de Baar, H. J. W.: Climatological mean and decadal change in surface ocean pCO_2 and net sea-air CO_2 flux over global oceans, Deep-Sea Res. Part II, 56, 554–577, doi:10.1016/j.dsr2.2008.12.009, 2009.

Takeda, S.: Influence of iron availability on nutrient consumption ratio of diatoms in oceanic waters, Nature, 393, 774–777, doi:10.1038/31674, 1998.

Timmermans, K. R., Veldhuis, M. J. W., Laan, P., and Brussaard, C. P. D.: Probing natural iron fertilization near the Kerguelen (Southern Ocean) using natural phytoplankton assemblages and diatom cultures, Deep-Sea Res. Part II, 55, 693–705, 2008.

Van Leeuwe, M. A., Scharek, R., de Baar, H. J. W., de jong, J. T. M., and Goeyens, L.: Iron enrichment experiments in the Southern Ocean: physiological responses of plankton communities, Deep-Sea Res. Part II, 44, 189–207, doi:10.1016/S0967.0645(96)00069-0, 1997.

Waldron, H. N., Attwood, C. G., Probyn, T. A., and Lucas, M. I.: Nitrogen dynamics in the Bellingshausen Sea during the Austral spring of 1992, Deep-Sea Res. Part II, 42, 1253–1276, 1995.

Ward, B. B.: Nitrification, in: Encyclopedia of Ecology, edited by: Jorgensen, S. E. and Faith, B. D., Ecological Processes, Vol 3 of Encyclopedia of Ecology, 5 vols. Elsevier, Oxford, 2511–2518, 2008.

Ward, B. B. and Zafiriou, O. C.: Nitrification and nitric oxide in the oxygen minimum of the eastern tropical north pacific, Deep-Sea Res., 35, 1127–1142, 1988.

Yool, A., Martin, A. P., Fernandez, C., and Clark, D. R.: The significance of nitrification for oceanic new production, Nature, 447, 999–1002, doi:10.1038/nature05885, 2007.